## Title
Computational Design of Stephenson II Six-Bar Function Generators for 11 Accuracy Points



**Journal**
Journal of Mechanisms and Robotics, 8(1)

**ISSN**
1942-4302

**Authors**
Plecnik, Mark M
McCarthy, J Michael

**Publication Date**
2016-02-01

**DOI**
10.1115/1.4031124

Peer reviewed

Journal of Mechanisms and Robotics. Received March 09, 2015;
Accepted manuscript posted July 23, 2015. doi:10.1115/1.4031124


# Computational Design of Stephenson II Six-bar Function Generators for 11 Accuracy Points

**Mark M. Plecnik**
Graduate Student Researcher
Email: mplecnik@uci.edu

**J. Michael McCarthy**
Professor
Email: mplecnik@uci.edu

Robotics and Automation Laboratory
Department of Mechanical and Aerospace Engineering
University of California, Irvine
Irvine, California 92697



*This paper presents a design methodology for Stephenson II six-bar function generators that coordinate 11 input and output angles. A complex number formulation of the loop equations yields 70 quadratic equations in 70 unknowns, which is reduced to system of 10 eighth degree polynomial equations of total degree* $8^{10} = 1.07 \times 10^9$. *These equations have a bilinear monomial structure, which yields a multi-homogeneous degree of 264,241,152. A sequence of polynomial homotopies is used to solve these equations and obtain 1,521,037 nonsingular candidate linkage designs. Each of these linkage candidates is evaluated to identify its cognates, and then analyzed to determine its input-output angles in each assembly. The result is a set of feasible linkage designs that reach the required accuracy points in a single assembly. As an example three Stephenson II function generators are designed that provide the input-output functions for the hip, knee, and ankle of a humanoid walking gait.*

## 1 Introduction

A function generator is a linkage that provides a specific position of the output link for a set of positions of the input link. This coordination of specific input-output joint parameters, termed accuracy points, is used in the design of "computing mechanisms" [1] to mechanically program a mathematical function. Six-bar function generators have been used in dwell mechanisms [2] and drive systems [3].

The additional design parameters in a six-bar linkage provide the opportunity to coordinate more accuracy points and achieve a more complex motion than a four-bar function generator, but this also means the system of polynomial design equations is much larger, [4] [5]. However, Plecnik and McCarthy [6] show that the ability to mechanically program the joint angles of a serial chain yields useful biomimetic movement with one degree-of-freedom. This is demonstrated in the example, where a one degree-of-freedom system is designed that achieves a humanoid walking gait.

## 2 Overview

This work focuses on the computational design of Stephenson II six-bar linkages for function generation. A Stephenson II linkage, Figure 1(a), is capable of coordinating 11 input-output angle pairs, called accuracy points. The synthesis formulation yields 70 quadratic equations in 70 unknowns, which are reduced to 10 eighth degree polynomials in 10 unknowns. Adding two homogeneous variables to these unknowns allows their separation into two sets of six homogeneous variables and the resulting equations are of fourth degree in each set of variables. The multihomogeneous degree of this polynomial system is 264,241,152.

These synthesis equations were solved by the polynomial homotopy solver BERTINI [7, 8], which implemented a regeneration module that ran for 311 hours on 256×2.2GHz processors on UC Irvine's High Performance Computing Cluster. Regeneration was used to solve a generic version of the synthesis equations to find 1,521,037 finite, nonsingular solutions. This solution set can be used to construct parameter homotopies that solve the synthesis equations for a required task in about two hours. The results are then analyzed according to a *performance verification* routine.

The large number of solutions to these design equations provide a rich array of linkage candidates. The evaluation of each candidate identifies feasible designs that provide the de-

Journal of Mechanisms and Robotics. Received March 09, 2015;
Accepted manuscript posted July 23, 2015. doi:10.1115/1.4031124


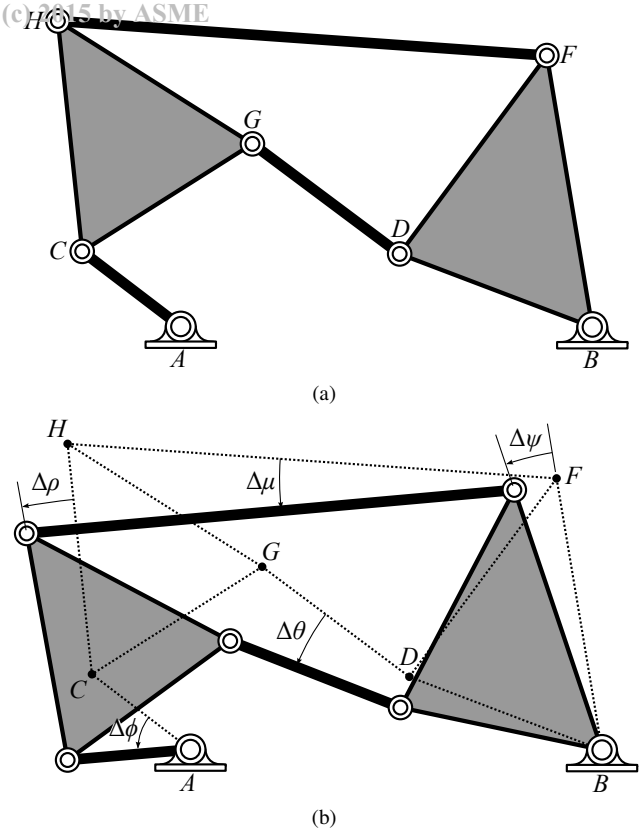


Fig. 1. (a) A Stephenson II linkage in its reference configuration and (b) a Stephenson II linkage displaced from its reference configuration drawn with dotted lines.

sired function to a high degree of accuracy. This is illustrated in the example.

## 3 Background

The design of a linkage to achieve a required set of input-output joint parameters is known as the kinematic synthesis of a function generator, [9–11]. Svoboda [1] designed function generators by fitting the input-output functions of a given set of linkages to the desired function. He patented a Watt II type six-bar linkage that computed a logarithmic function [12]. Freudenstein [4] introduced a new approach that used the loop equations of a four-bar linkage to fit a given set of accuracy points to obtain a four-bar function generator.

McLarnan [13] formulated the loop equations for a Stephenson II function generator and found some solutions for eight positions using the Newton-Raphson method. Mohan Rao et al. [14] used principles of Burmester theory to design six-bar linkages that perform simultaneous function and path generation. Dhingra et al. [5] solved the synthesis equations for nine accuracy positions using a polynomial homotopy algorithm. Liu et al. [15] used homotopy to solve for six-bar function generators that coordinate five positions, then used the solutions as start points for optimal synthesis, noting the problem of linkage defects. Simionescu and Alexandru [16] approached the optimal synthesis of Stephenson linkages by removing one link, and considering the 2 degree-of-freedom displacement equations to formulate an objective function. Akçali [17] adopted a modular approach to the optimal synthesis of six-bar function generators.

Kinzel et al. [18] used parametric design software to graphically synthesize an 11 position six-bar function generator. Hwang and Chen [19] formulated the design of Stephenson II six-bar function generators fusing optimization techniques to find defect-free linkages. Sancibrian [20] used a similar approach to find the linkage parameters that minimize the difference between the input-output function of the linkage and the desired function. Plecnik and McCarthy [21] used homotopy to find solution sets for eight position function generators.

In this paper, we formulate complex versions of the loop equations of a Stephenson II six-bar linkage and solve them directly using a homotopy technique called *regeneration* [8]. The result was over a million candidate linkage solutions, where were then used to construct parameter homotopies to efficiently calculate Stephenson II function generators that coordinate specified sets of 11 input-output angles.

Each candidate linkage design is analyzed to determine if it passes through the specified task in one configuration and without passing through a singularity. This requires identification of six-bar cognates [23], and sorting each of the assemblies of the large number candidate linkage designs. The example shows that this design procedure yielded as many as 50 useful Stephenson II six-bar linkages that achieve complex functions used to model leg movement.

## 4 Complex Numbers

Erdman et al. [10] show that complex numbers provide a convenient formulation of planar kinematics. A point $P = (P_x, P_y)$ can be represented as the complex number,

$$P = P_x + iP_y. \tag{1}$$

The component-wise sum of a complex number is the same as for coordinate vectors, and the product of complex numbers performs rotation and scaling operations. In particular, the exponential $e^{i\theta}$ is a rotation operator on complex numbers that yields the same result as a $2\times2$ rotation matrix operating on vectors, that is,

$$\begin{aligned} P &= e^{i\theta} p, \\ P_x + iP_y &= (\cos\theta + i\sin\theta)(p_x + ip_y), \\ P_x + iP_y &= (\cos\theta p_x - \sin\theta p_y) + i(\sin\theta p_x + \cos\theta p_y). \end{aligned} \tag{2}$$

Wampler [22] shows that it is convenient to formulate planar kinematics equations in terms of the complex numbers and their conjugates, termed *isotropic coordinates*. Note that a rotation operator $T = e^{i\theta}$ and its conjugate $\bar{T} = e^{-i\theta}$ should have unit magnitude and satisfy the normalization condition,

$$T\bar{T} = 1. \tag{3}$$

Journal of Mechanisms and Robotics. Received March 09, 2015;
Accepted manuscript posted July 23, 2015. doi:10.1115/1.4031124


In the following derivations, this provides a symmetric structure to the synthesis equations that is exploited to simplify these equations.

## 5 Synthesis Equations for the Stephenson II

A Stephenson II linkage is shown in Figure 1(a). It is defined by the coordinates of seven pivots $A$, $B$, $C$, $D$, $F$, $G$, and $H$ which mark the reference configuration of the linkage. These pivots connect to form five moving links $AC$, $CGH$, $BDF$, $DG$, and $FH$. Moving the mechanism from its reference configuration, the orientation of each displaced link is measured by $\Delta\phi$, $\Delta\rho$, $\Delta\psi$, $\Delta\theta$, and $\Delta\mu$, respectively, see Figure 1(b). Moving the mechanism to its $j^{\text{th}}$ configuration, each angle is used to define the complex rotation operators $Q_j$, $R_j$, $S_j$, $T_j$, and $U_j$,

$$\begin{aligned} Q_j &= e^{i\Delta\phi_j}, \qquad R_j = e^{i\Delta\rho_j}, \qquad S_j = e^{i\Delta\psi_j}, \\ T_j &= e^{\Delta\theta_j}, \qquad U_j = e^{\Delta\mu_j}, \qquad j = 1,\ldots,N-1. \end{aligned} \tag{4}$$

The synthesis objective is to find the pivot locations of a Stephenson II linkage that coordinates the angles of links $AC$ and $BDF$ at $N$ positions $(\Delta\phi_j, \Delta\psi_j)$, $j = 0,\ldots,N-1$, see Figure 2. In order to set the scale, orientation, and location of the linkage in the plane, the locations of ground pivots $A$ and $B$ are specified, leaving the moving pivots $C$, $D$, $F$, $G$, $H$ as the unknowns to be solved.

In order to form the loop equations, we first write the positions of pivots $D$, $F$, $G$,and $H$, in the $j^{\text{th}}$ configuration, see Fig . 2(b),

$$\begin{aligned} D_j &= B + S_j(D-B), \\ F_j &= B + S_j(F-B), \\ G_j &= A + Q_j(C-A) + R_j(G-C), \\ H_j &= A + Q_j(C-A) + R_j(H-C), \qquad j = 1,\ldots,N-1. \end{aligned} \tag{5}$$

The loop equations for the Stephenson II six-bar linkage are obtained by evaluating $G_j - D_j$ and $H_j - F_j$ relative to the initial configuration. This yields two sets of complex conjugate loop equations,

$$\begin{aligned} \mathcal{L}_j : T_j(G-D) &= \\ &(A + Q_j(C-A) + R_j(G-C)) - (B + S_j(D-B)), \\ \bar{T}_j(\bar{G}-\bar{D}) &= \\ &(\bar{A} + \bar{Q}_j(\bar{C}-\bar{A}) + \bar{R}_j(\bar{G}-\bar{C})) - (\bar{B} + \bar{S}_j(\bar{D}-\bar{B})), \\ &\qquad j = 1,\ldots,N-1, \\ \mathcal{M}_j : U_j(H-F) &= \\ &(A + Q_j(C-A) + R_j(H-C)) - (B + S_j(F-B)), \\ \bar{U}_j(\bar{H}-\bar{F}) &= \\ &(\bar{A} + \bar{Q}_j(\bar{C}-\bar{A}) + \bar{R}_j(\bar{H}-\bar{C})) - (\bar{B} + \bar{S}_j(\bar{F}-\bar{B})), \\ &\qquad j = 1,\ldots,N-1. \end{aligned} \tag{6}$$

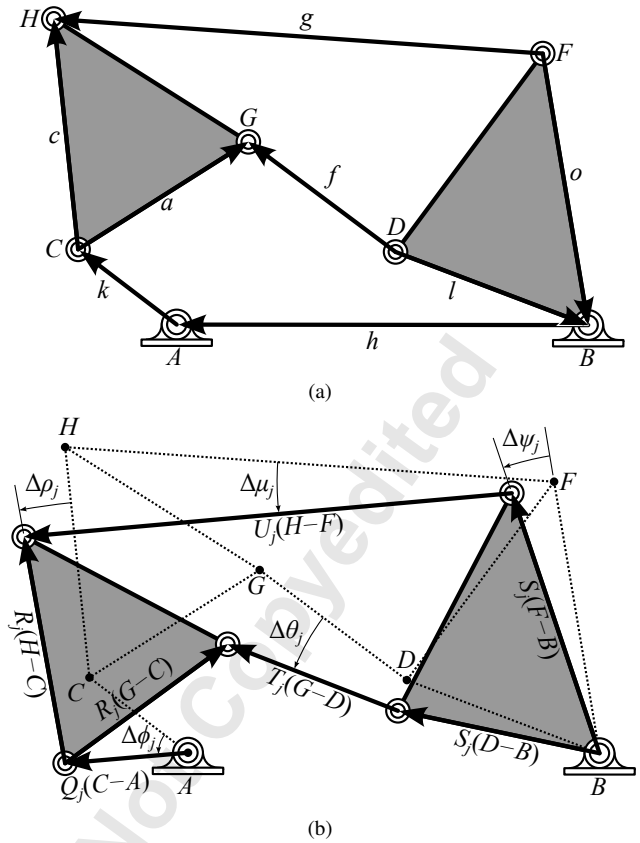


Fig. 2. (a) Link vectors of the Stephenson II linkage and (b) link vectors in the $j^{\text{th}}$ displaced configuration.

The rotation operators $Q_j$, $\bar{Q}_j$, $S_j$ and $\bar{S}_j$ are defined by the task function which is selected by the designer. The remaining joint variables $R_j$, $\bar{R}_j$, $T_j$, $\bar{T}_j$, $U_j$, and $\bar{U}_j$ must satisfy the normalization conditions,

$$R_j\bar{R}_j = 1, \quad T_j\bar{T}_j = 1, \quad U_j\bar{U}_j = 1, \quad j = 1,\ldots,N-1. \tag{7}$$

The loop equations $\mathcal{L}_j$, $\mathcal{M}_j$ and the normalization conditions (7) form $7(N-1)$ quadratic equations in the $10+6(N-1)$ unknowns which consist of the pivots $C$, $D$, $F$, $G$ and $H$ and the joint rotations $R_j$, $T_j$ and $U_j$ and their complex conjugates. In this work, we explore the square case $N = 11$ when the number of equations and unknowns are equal so that a finite set of isolated solution points can be computed. For this case, there are 70 quadratic equations and 70 unknowns forming a system of degree $2^{70} = 1.18 \times 10^{21}$.

## 6 Simplification of the Synthesis Equations

The 70 synthesis equations for the Stephenson II function generator can be reduced to 10 equations in 10 unknowns in a sequence of three steps. First, solve for $T_j$ and $\bar{T}_j$ in the pairs of equations $\mathcal{L}_j$ of (6), and substitute the result into the normalization conditions $T_j\bar{T}_j = 1$. Second solve for $U_j$ and $\bar{U}_j$ in the pairs of equations $\mathcal{M}_j$ of (6), and substitute into the normalization conditions $U_j\bar{U}_j = 1$. Finally, these two steps yield 10 pairs of equations that are linear in the

Journal of Mechanisms and Robotics. Received March 09, 2015;
Accepted manuscript posted July 23, 2015. doi:10.1115/1.4031124


joint variables $R_j$ and $\bar{R}_j$, which can be computed and then substituted into the normalization condition, $R_j\bar{R}_j = 1$.

To simplify the presentation of this calculation, introduce the link vectors,

$$\begin{aligned} a &= G - C, \quad f = G - D, \quad h = A - B, \quad l = -(D - B), \\ c &= H - C, \quad g = H - F, \quad k = C - A, \quad o = -(F - B), \end{aligned} \tag{8}$$

which are drawn in Figure 2(a). Then rearrange the equations to obtain,

$$\begin{aligned} \mathcal{L}_j: \quad & h + Q_j k + R_j a + S_j l - T_j f = 0, \\ & \bar{h} + \bar{Q}_j \bar{k} + \bar{R}_j \bar{a} + \bar{S}_j \bar{l} - \bar{T}_j \bar{f} = 0, \quad j = 1, \ldots, 10, \\ \mathcal{M}_j: \quad & h + Q_j k + R_j c + S_j o - U_j g = 0, \\ & \bar{h} + \bar{Q}_j \bar{k} + \bar{R}_j \bar{c} + \bar{S}_j \bar{o} - \bar{U}_j \bar{g} = 0, \quad j = 1, \ldots, 10. \end{aligned} \tag{9}$$

Eliminate $T_j$ and $\bar{T}_j$ in $\mathcal{L}_j$ of (9) and $U_j$ and $\bar{U}_j$ in $\mathcal{M}_j$ of (6) to obtain the pairs of equations,

$$\begin{aligned} &(h + Q_j k + R_j a + S_j l)(\bar{h} + \bar{Q}_j \bar{k} + \bar{R}_j \bar{a} + \bar{S}_j \bar{l}) = f\bar{f}, \\ &(h + Q_j k + R_j c + S_j o)(\bar{h} + \bar{Q}_j \bar{k} + \bar{R}_j \bar{c} + \bar{S}_j o) = g\bar{g}, \\ &\qquad j = 1, \ldots, 10. \end{aligned} \tag{10}$$

Expand these equations to obtain 10 pairs of equations that are linear in $R_j$ and $\bar{R}_j$, that can be written in the form,

$$\begin{bmatrix} a\bar{b}_j & \bar{a}b_j \\ c\bar{d}_j & \bar{c}d_j \end{bmatrix} \begin{Bmatrix} R_j \\ \bar{R}_j \end{Bmatrix} = \begin{Bmatrix} f\bar{f} - a\bar{a} - b_j\bar{b}_j \\ g\bar{g} - a\bar{a} - d_j\bar{d}_j \end{Bmatrix}, j = 1, \ldots, 10, \tag{11}$$

where the vectors $b_j = C_j - D_j$ and $d_j = C_j - F_j$ given by

$$\begin{aligned} b_j &= h + Q_j k + S_j l, \\ d_j &= h + Q_j k + S_j o, \\ & \qquad j = 1, \ldots, 10, \end{aligned} \tag{12}$$

are introduced to simplify presentation of the equations.

Solve for $R_j$ and $\bar{R}_j$ and substitute into $R_j\bar{R}_j = 1$ to obtain the 10 synthesis equations,

$$\begin{aligned} &(a\bar{b}_j(g\bar{g} - c\bar{c} - d_j\bar{d}_j) - c\bar{d}_j(f\bar{f} - a\bar{a} - b_j\bar{b}_j)) \\ &\quad \times (\bar{a}b_j(g\bar{g} - c\bar{c} - d_j\bar{d}_j) - \bar{c}d_j(f\bar{f} - a\bar{a} - b_j\bar{b}_j)) \\ &\quad + (a\bar{b}_j\bar{c}d_j - \bar{a}b_j c\bar{d}_j)^2 = 0, \qquad j = 1, \ldots, 10. \end{aligned} \tag{13}$$

These equations are of degree eight in the 10 design parameters formed by $C$, $D$, $F$, $G$, $H$, and their conjugates $\bar{C}$, $\bar{D}$, $\bar{F}$, $\bar{G}$, $\bar{H}$. The total degree of this polynomial system is $8^{10} = 1.07 \times 10^9$.

These equations can be separated into two groups,

$$\langle C, D, F, G, H \rangle, \quad \langle \bar{C}, \bar{D}, \bar{F}, \bar{G}, \bar{H} \rangle. \tag{14}$$

A homogeneous variable is added to each group so that the synthesis equations are separately homogeneous to the fourth degree in each set of variables.

The root count for a set of polynomials with this biquartic monomial structure is obtained by expanding the binomial,

$$(4\alpha_1 + 4\alpha_2)^{10}, \tag{15}$$

and selecting the coefficient of the term $\alpha_1^5\alpha_2^5$ defined by the two sets of five parameters. The result is the multihomogeneous degree of $264,241,152$.

## 7 Solution of the Synthesis Equations

The synthesis equations (13) were solved using BERTINI for a random set of complex numbers assigned to the parameters $(Q_j, S_j)$, $j = 1, \ldots, 10$, in order to find a general set of solutions that can be used to form a parameter homotopy. A homotopy method called regeneration was implemented that solves this system incrementally.

Regeneration tracks solutions for several levels of homotopies. In a square system of $n$ equations and unknowns, the first level solves a system composed of 1 equation of the target system and $n-1$ arbitrarily specified linear equations in all unknowns. The finite isolated solutions of the first level are used to solve the second level system. At each succeeding level, one linear equation is replaced with one target system equation until the final level when the target system is solved. A more detailed description of regeneration is found in Bates et al. [8].

The regeneration homotopy required 311 hrs on 256 cores processing at 2.2 GHz to compute, and tracked 24,822,328 paths over 10 levels to find 1,521,037 nonsingular solutions. These nonsingular solutions can be used to construct parameter homotopies for efficient calculation of linkage solutions for a specific sets of 11 coordinated joint angles.

Parameter homotopies use the nonsingular solutions of a generic member of a family of polynomial systems to find the nonsingular solutions of any other member in that family. Each member $\mathbf{f}(\mathbf{z}, \mathbf{q})$ contains the set of variables $\mathbf{z}$ and is defined by a set of parameters $\mathbf{q}$. If all the nonsingular solutions of a general system $\mathbf{f}(\mathbf{z}, \mathbf{q}_{\text{gen}})$ are known, they can be used as startpoints that track to all the nonsingular solutions of a specific system $\mathbf{f}(\mathbf{z}, \mathbf{q}_{\text{spec}})$. The computational benefit of parameter homotopy is that it avoids tracking paths that have endpoints at infinity. A more detailed description of parameter homotopy is found in Bates et al. [8].

## 8 Sorting Solutions

The solutions of the synthesis equations are examined to identify design candidates. Design candidates are those

Journal of Mechanisms and Robotics. Received March 09, 2015;
Accepted manuscript posted July 23, 2015. doi:10.1115/1.4031124


solutions which correspond to physical linkages and were analyzed to verify performance. For each design candidate, there will exist two synthesis solutions that arise from interchanging the pivot labels of coupler links $DG$ and $FH$. Furthermore, design candidates are all members of function generator cognate sets of three.

In order to check whether a solution corresponds to a physical linkage, we check that each variable and its calculated conjugate are actually complex conjugates. Within this set, we find solution pairs with values of floating coupler pivots $\{D,G\}$ and $\{F,H\}$ interchanged. We choose one solution from each pair to analyze because they redundantly correspond to the same linkage. Finally, we sort design candidates into cognate triples according to equation (20) below.

### 8.1 Cognates

Function generator cognates are linkages of the same kinematic structure, but with different link length ratios, that produce an identical coordination of input-output angles [23, 24]. Every Stephenson II linkage has two other function cognates. Therefore, our synthesis results can be sorted into triples of function cognates. However, it can happen that a cognate solution may not be found due to numerical error. In these cases, cognates are constructed and added to the synthesis results.

A Stephenson II function generator with specified ground pivots $A$ and $B$ has cognates defined by the four-bar linkage that forms the floating loop $DGHF$, see Figure 3. To see this, note that the movement of pivot $C$ relative to Link $BDF$ creates a path that is traced by the coupler link of four-bar $DGHF$ that is attached to Link $BDF$. Therefore, all four-bar linkages that generate the same coupler curve of $C$ relative to link $BDF$ can replace $DGHF$ and still control links $AC$ and $BDF$ in the same manner. The Roberts–Chebyshev theorem states that for a four-bar linkage that traces a coupler curve, there will exist two other four-bars that trace that same coupler curve [25]. Therefore, there exists three Stephenson II linkages that produce identical functions.

The set of four-bar linkages that guide a point $C$ along the same curve are called path generator cognates of the four-bar linkage. Figure 4 shows four-bars $DGHF$, $DG'H'F'$, and $F'G''H''F$ as path generator cognates connected in an overconstrained mechanism that guides shared point $C$. The three four-bar path generator cognates are used to construct three Stephenson II six-bar function generator cognates, allowing the synthesis solutions to be sorted into cognate triples.

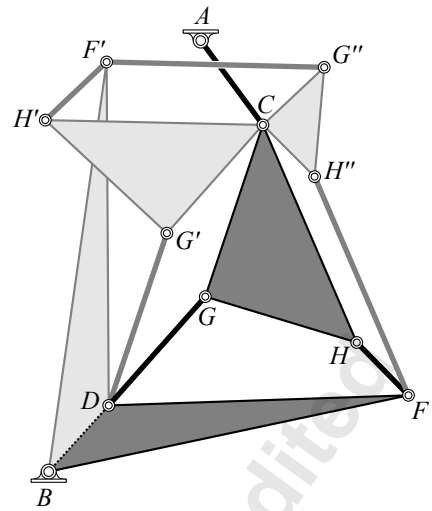


Fig. 3. Three Stephenson II cognate function generators shown in a single overconstrained mechanism. The three cognate mechanisms are comprised of pivots $\{A,B,C,D,G,H,F\}$, $\{A,B,C,D,G',H',F'\}$, and $\{A,B,C,F',G'',H'',F\}$.

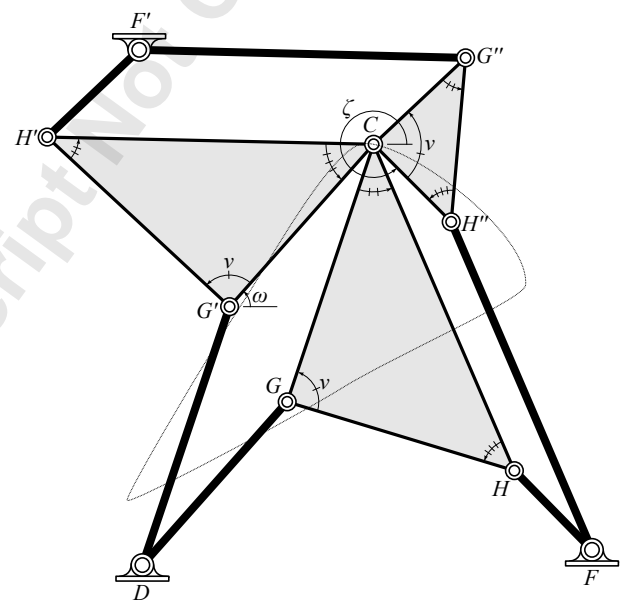


Fig. 4. The coupler curve traced by $C$ as part of the four-bar $DGHF$ is the same for two additional cognate linkages $DG'H'F'$ and $F'G''H''F$.

### 8.2 Constructing the Cognates

In this section, we construct two function generator cognates from a Stephenson II linkage defined by the design candidate $\{A,B,C,D,G,H,F\}$, see Fig 3. This construction is based on that of the four-bar path generator cognates, see Figure 4.

Figure 4 depicts parallelograms $DGCG'$, $FHCH''$, $F'H'CG''$, and similar triangles $\triangle CGH$, $\triangle H'G'C$, and $\triangle G''CH''$. Each triangles contains the angle $\nu$ that is $\angle CGH$, $\angle H'G'C$, and $\angle G''CH''$. The vector $C-G'$ is rotated by $\omega$ from horizontal, and the vector $H''-C$ is rotated by $\zeta$ from horizontal. The angles $\nu$, $\omega$, and $\zeta$ define rotation operators $V$, $W$, and $Z$,

$$V = e^{i\nu}, \qquad W = e^{i\omega}, \qquad Z = e^{i\zeta}. \tag{16}$$

The cognate pivot locations $G'$, $H''$, $H'$, $G''$, $F'$ can be written

Journal of Mechanisms and Robotics. Received March 09, 2015;
Accepted manuscript posted July 23, 2015. doi:10.1115/1.4031124


as

$$\begin{aligned}
G' &= D + (C - G),\\
H'' &= F + (C - H),\\
H' &= G' + WV|H' - G'|,\\
G'' &= C + ZV|G'' - C|,\\
F' &= H' + (G'' - C).
\end{aligned} \tag{17}$$

The rotation operators can be computed as

$$V = \sqrt{\frac{(C-G)(\bar{H}-\bar{G})}{(\bar{C}-\bar{G})(H-G)}},\quad W = \sqrt{\frac{C-G'}{\bar{C}-\bar{G}'}},\quad Z = \sqrt{\frac{H''-C}{\bar{H}''-\bar{C}}}, \tag{18}$$

which is substituted into equation (17) in order to write the cognate pivots in terms of the original four-bar pivots,

$$\begin{aligned}
G' &= D - G + C,\\
H'' &= F - H + C,\\
H' &= \left(\frac{D-G}{H-G}\right)(H-C) + C,\\
G'' &= \left(\frac{F-H}{G-H}\right)(G-C) + C,\\
F' &= \frac{(D-G)(H-C) - (F-H)(G-C)}{H-G} + C.
\end{aligned} \tag{19}$$

The two four-bars $DG'H'F'$ and $F'G''H''F$ are cognates of $DGHF$. Following this, a Stephenson II function generator with pivots $A$, $B$, $C$ and floating four-bar loop $DGHF$ will have two function generator cognates. The cognate pivots are given by solution pairs,

$$\begin{aligned}
(DGHF)_{c1} &= DG'H'F',\ \ F'H'G'D,\\
(DGHF)_{c2} &= F'G''H''F,\ \ FH''G''F'.
\end{aligned} \tag{20}$$

These solution pairs arise because a single Stephenson II design will correspond to two synthesis solutions where the values of floating pivot locations $\{D,G\}$ and $\{F,H\}$ are interchanged. Equation (20) is used to sort cognate triples from the linkage design candidates. If a cognate is found to be missing from the design candidates, it is added.

## 9 Performance Verification of a Candidate Linkage

Once the linkage design candidates have been sorted into solution pairs and cognate triples, they are analyzed to evaluate the performance of each design. The criteria for a feasible design is that all of the accuracy points are reached on one trajectory of configurations, known as an assembly. Chase and Mirth [26] and Balli and Chand [27] refer to linkages that do not satisfy this requirement as having a *circuit defect*.

In addition, we require that the determinant of the Jacobian of the loop equations not pass through zero along the configuration trajectory. These are known as *singular configurations* and a linkage that passes through a singularity is said to have a *branch defect* [26].

Thus, our goal is to identify for each design candidate, whether there is a configuration trajectory that includes all of the accuracy points and does not include a singularity. In other words, the linkage does not have circuit or branch defects.

### 9.1 Analysis of each design candidate

The kinematics equations of the Stephenson II linkage, equation (6), can be assembled in the form,

$$\begin{aligned}
L =& T(G-D) - (A + Q(C-A) + R(G-C))\\
&+ (B + S(D-B)) = 0,\\
\bar{L} =& \bar{T}(\bar{G}-\bar{D}) - (\bar{A} + \bar{Q}(\bar{C}-\bar{A}) + \bar{R}(\bar{G}-\bar{C}))\\
&+ (\bar{B} + \bar{S}(\bar{D}-\bar{B})) = 0,\\
M =& U(H-F) - (A + Q(C-A) + R(H-C))\\
&+ (B + S(F-B)) = 0,\\
\bar{M} =& \bar{U}(\bar{H}-\bar{F}) - (\bar{A} + \bar{Q}(\bar{C}-\bar{A}) + \bar{R}(\bar{H}-\bar{C}))\\
&+ (\bar{B} + \bar{S}(\bar{F}-\bar{B})) = 0,
\end{aligned} \tag{21}$$

which include the constant initial pivot locations,

$$\{A,\bar{A},B,\bar{B},C,\bar{C},D,\bar{D},F,\bar{F},G,\bar{G},H,\bar{H}\}, \tag{22}$$

and the variable joint angle parameters,

$$\{Q,\bar{Q},R,\bar{R},S,\bar{S},T,\bar{T},U,\bar{U}\}. \tag{23}$$

In the case that binary link angle $\phi$ is the input parameter, then the input $\mathbf{x}$ and output $\mathbf{y}$ variables are

$$\mathbf{x} = (Q,\bar{Q}),\quad \mathbf{y} = (R,\bar{R},S,\bar{S},T,\bar{T},U,\bar{U}), \tag{24}$$

and the analysis equations are

$$\mathbf{F}(\mathbf{x},\mathbf{y}) = \begin{Bmatrix} L\\ \bar{L}\\ M\\ \bar{M}\\ R\bar{R}-1\\ S\bar{S}-1\\ T\bar{T}-1\\ U\bar{U}-1 \end{Bmatrix} = \begin{Bmatrix} 0\\ 0\\ 0\\ 0\\ 0\\ 0\\ 0\\ 0 \end{Bmatrix}. \tag{25}$$

These equations have six solutions for a specified input $\mathbf{x} = (Q,\bar{Q})$ and are easily solved using the *NSolve* function in MATHEMATICA. In the case that ternary link angle $\psi$ is the

Journal of Mechanisms and Robotics. Received March 09, 2015;
Accepted manuscript posted July 23, 2015. doi:10.1115/1.4031124


input parameter, then $\mathbf{x} = (S, \bar{S})$ and equations (24) and (25) change appropriately. The choice of input link provides different parameterizations of the same configuration space and will define different sets of singular configurations. Singular configurations are locations in the configuration space where $\det[J_{\mathbf{F}}(\mathbf{x},\mathbf{y})] = 0$,

$$[J_{\mathbf{F}}(\mathbf{x},\mathbf{y})] = \left[\frac{\partial \mathbf{F}}{\partial y_1}, \ldots, \frac{\partial \mathbf{F}}{\partial y_8}\right]. \tag{26}$$

Singular configurations define the bounds of mechanism branches.

### 9.2 Sorting the linkage configurations

A set of input parameters $\mathbf{x}_k$, $k = 1, \ldots, n$ is generated that sweeps around the unit circle,

$$\mathbf{x}_k = \left\{\exp\left((i2\pi)\frac{k-1}{n-1}\right), \exp\left(-(i2\pi)\frac{k-1}{n-1}\right)\right\}, \quad k = 1, \ldots, n. \tag{27}$$

Equations (25) are solved for each $\mathbf{x}_k$ to generate $n$ sets of configurations,

$$\mathcal{C}_k = \{(\mathbf{x}_k, \mathbf{y}_{k,1}), \ldots, (\mathbf{x}_k, \mathbf{y}_{k,6})\}, \quad k = 1, \ldots, n. \tag{28}$$

The members of $\mathcal{C}_k$ for each $k$ appear in no particular order, and the goal of this section is to sort configurations into separate trajectories as we increment $k$ from 1 to $n$.

The algorithm initializes by setting the six elements of $\mathcal{C}_1$ as the beginning of six trajectories which are built upon by comparing $\mathcal{C}_k$ to $\mathcal{C}_{k+1}$ and deciphering pairs of connecting configurations,

$$\begin{aligned} \mathcal{C}_k &= \{(\mathbf{x}_k, \mathbf{y}_{k,p}) \mid p = 1, \ldots, 6\}, \\ \mathcal{C}_{k+1} &= \{(\mathbf{x}_{k+1}, \mathbf{y}_{k+1,q}) \mid q = 1, \ldots, 6\}, \end{aligned} \tag{29}$$

where in general configurations $(\mathbf{x}_k, \mathbf{y}_{k,p})$ and $(\mathbf{x}_{k+1}, \mathbf{y}_{k+1,q})$ connect such that $p \neq q$. To decipher connections between $\mathcal{C}_k$ and $\mathcal{C}_{k+1}$, we use Newton's method to solve $\mathbf{F}(\mathbf{x}_{k+1}, \mathbf{y}) = 0$ for $\mathbf{y}$ using start points $\mathbf{y}_{k,p}$, for $p = 1, \ldots, 6$. We name these approximate solutions $\tilde{\mathbf{y}}_{k+1,p}$ where,

$$\tilde{\mathbf{y}}_{k+1,p} = \mathbf{y}_{k,p} - [J_{\mathbf{F}}(\mathbf{x}_{k+1}, \mathbf{y}_{k,p})]^{-1}\mathbf{F}(\mathbf{x}_{k+1}, \mathbf{y}_{k,p}), \quad p = 1, \ldots, 6, \tag{30}$$

is calculated from a single Newton iteration. Multiple iterations are used for more accuracy. The approximate configuration set $\tilde{\mathcal{C}}_{k+1}$ is formed from $\tilde{\mathbf{y}}_{k+1,p}$ where

$$\tilde{\mathcal{C}}_{k+1} = \{(\mathbf{x}_{k+1}, \tilde{\mathbf{y}}_{k+1,p}) \mid p = 1, \ldots, 6\}. \tag{31}$$

Configuration $(\mathbf{x}_k, \mathbf{y}_{k,p})$ of $\mathcal{C}_k$ connects to configuration $(\mathbf{x}_{k+1}, \mathbf{y}_{k+1,q})$ of $\mathcal{C}_{k+1}$ if the following condition evaluates as true,

$$|\tilde{\mathbf{y}}_{k+1,p} - \mathbf{y}_{k+1,q}| < \text{tol}, \tag{32}$$

where tol is a specified threshold value. For most $k$, configurations $\mathcal{C}_k$ and $\mathcal{C}_{k+1}$ will connect in a one to one fashion. However, equation (32) allows the possibility that a configuration of $\mathcal{C}_k$ will connect to several or none of the configurations of $\mathcal{C}_{k+1}$, which is often the case near singularities. In these cases, we employ the following logic:

1. If a configuration of $\mathcal{C}_{k+1}$ is not connected to a configuration of $\mathcal{C}_k$, that configuration of $\mathcal{C}_{k+1}$ begins a new trajectory.
2. If a configuration of $\mathcal{C}_k$ connects to multiple configurations of $\mathcal{C}_{k+1}$, the trajectory associated with the configuration of $\mathcal{C}_k$ is duplicated and each duplicate connects to a matching element of $\mathcal{C}_{k+1}$.
3. If a configuration of $\mathcal{C}_k$ does not connect to any configurations of $\mathcal{C}_{k+1}$, the trajectory associated with the configuration of $\mathcal{C}_k$ is concluded.

This procedure is executed for a complete sweep of the unit circle $\mathbf{x}_k$, $k = 1, \ldots, n$, such that $\mathbf{x}_n = \mathbf{x}_1$. The result of this algorithm is a set of connected sequences of configurations that form separate mechanism trajectories. All combinations of these trajectories are checked for connections from $k = n$ to $k = 1$ configurations. If connections are identified, these trajectories are chained together to form longer trajectories.

Finally, configurations that do not correspond to rigid body movement are removed, and the determinant of the Jacobian matrix along each configuration is evaluated. A sign change indicates a change in configuration that can arise from numerical error.

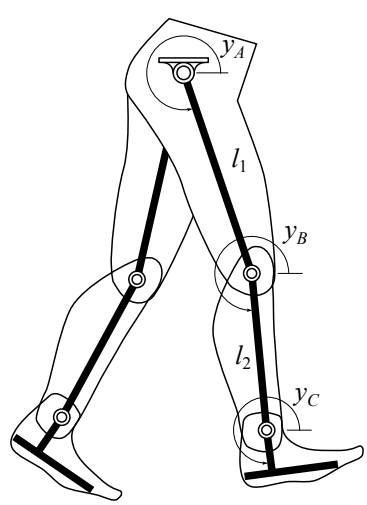


Fig. 5. A humanoid leg is modelled as a planar 3R chain where $l_1 = 18.7$ and $l_2 = 14$.

Journal of Mechanisms and Robotics. Received March 09, 2015;
Accepted manuscript posted July 23, 2015. doi:10.1115/1.4031124


Table 1. Fourier coefficients for walking gait joint angle functions.

| | Hip: $f_A(t)$ | Knee: $f_B(t)$ | Ankle: $f_C(t)$ |
|---|---|---|---|
| $o$ | 3 | 5 | 5 |
| $a_0$ | −0.23899606 | −0.42317334 | −0.39916633 |
| $a_1$ | 0.26507432 | 0.16530352 | 0.24817028 |
| $b_1$ | 0.04632108 | 0.38229515 | 0.34926232 |
| $a_2$ | 0.00265777 | 0.20929088 | 0.10641896 |
| $b_2$ | −0.05632819 | 0.12673270 | 0.10372243 |
| $a_3$ | −0.02058442 | 0.04930281 | 0.02732644 |
| $b_3$ | 0.01472108 | 0.04075846 | 0.09697237 |
| $a_4$ | 0 | 0.00107466 | 0.01722405 |
| $b_4$ | 0 | 0.01778866 | 0.00426672 |
| $a_5$ | 0 | 0.00429589 | −0.01269033 |
| $b_5$ | 0 | 0.00522743 | −0.01612253 |

Table 2. Task points for each example function. Values below are given in degrees and must be converted to radians in order for $f_A(t)$, $f_B(t)$, and $f_C(t)$ to evaluate properly.

| $j$ | Hip | Knee | Ankle |
|---|---|---|---|
| 0 | $(0, 0)$ | $(0, 0)$ | $(0, 0)$ |
| 1 | $(50, f_A(50))$ | $(25, f_B(25))$ | $(32, f_C(32))$ |
| 2 | $(85, f_A(85))$ | $(60, f_B(60))$ | $(65, f_C(65))$ |
| 3 | $(125, f_A(125))$ | $(94, f_B(94))$ | $(94, f_C(94))$ |
| 4 | $(165, f_A(165))$ | $(152, f_B(152))$ | $(146, f_C(146))$ |
| 5 | $(212, f_A(212))$ | $(202, f_B(202))$ | $(188, f_C(188))$ |
| 6 | $(244, f_A(244))$ | $(237, f_B(237))$ | $(226, f_C(226))$ |
| 7 | $(261, f_A(261))$ | $(278, f_B(278))$ | $(264, f_C(264))$ |
| 8 | $(278, f_A(278))$ | $(313, f_B(313))$ | $(297, f_C(297))$ |
| 9 | $(297, f_A(297))$ | $(331, f_B(331))$ | $(327, f_C(327))$ |
| 10 | $(327, f_A(327))$ | $(346, f_B(346))$ | $(344, f_C(344))$ |

### 9.3 Identifying feasible designs

Once all trajectories have been assembled for a linkage design candidate, they are each checked to see which and how many of the specified accuracy points they contain. A feasible design produces a trajectory that moves through all 11 accuracy points in one assembly. We term these designs 11-point mechanisms.

While linkage designs that contain all 11 accuracy points on a single trajectory is the goal, our design process identifies linkages with trajectories that move through less than 11 points as well. In this work, we keep track of 9- and 10-point mechanisms, too. It is often the case that these mechanisms will slightly miss some accuracy points, and may have other features useful to the designer, such as compact dimensions or reduced link overlap.

Table 3. Synthesis results when (a) the binary link is chosen as the input and (b) the ternary link is chosen as the input.

(a) Input $\phi_A = \phi_B = \phi_C = t$.

| | $\Delta y_A$ | $\Delta y_B$ | $\Delta y_C$ |
|---|---|---|---|
| Linkage solutions | 14,445 | 8,255 | 9,835 |
| Design candidates | 6,686 | 3,830 | 4,791 |
| 11-point mechanisms | 0 | 0 | 0 |
| 10-point mechanisms | 2 | 0 | 0 |
| 9-point mechanisms | 78 | 27 | 17 |
| Synthesis computation time (hr) | 2.9 | 2.0 | 2.0 |
| Analysis computation time (hr) | 9.4 | 5.2 | 6.4 |

(b) Input $\psi_A = \psi_B = \psi_C = t$.

| | $\Delta y_A$ | $\Delta y_B$ | $\Delta y_C$ |
|---|---|---|---|
| Linkage solutions | 11,175 | 11,459 | 9,913 |
| Design candidates | 4,496 | 5,100 | 4,636 |
| 11-point mechanisms | 51 | 28 | 6 |
| 10-point mechanisms | 119 | 144 | 13 |
| 9-point mechanisms | 129 | 183 | 26 |
| Synthesis computation time (hr) | 2.1 | 1.5 | 1.7 |
| Analysis computation time (hr) | 6.3 | 7 | 6.1 |

## 10 Hip, Knee, and Ankle Function Generators

In order to illustrate this design procedure, we specify functions for the movement of the hip, knee, and ankle joints of a humanoid walking gait, see Figure 5, and design Stephenson II function generators to generate these functions from a single constant velocity input. The joint functions were obtained from a video of a walking movement. The resulting joint functions have asymmetries that test the performance of this design system for six-bar function generators, see Figure 6.

The angles at the hip $y_A$, knee $y_B$, and ankle $y_C$ shown in Figure 5 are given by

$$\begin{aligned} y_A &= f_A(t) - 71^\circ, \\ y_B &= f_B(t) - 84.95^\circ, \\ y_C &= f_C(t) - 82.45^\circ, \end{aligned} \tag{33}$$

where the three functions $f_A(t)$, $f_B(t)$, and $f_C(t)$ are periodic

Journal of Mechanisms and Robotics. Received March 09, 2015;
Accepted manuscript posted July 23, 2015. doi:10.1115/1.4031124


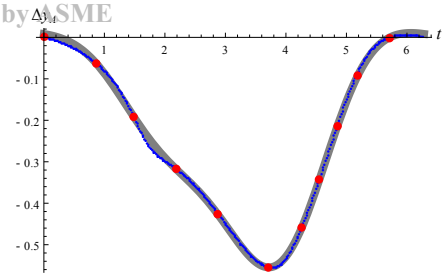


(a) Hip joint function $\Delta y_A = f_A(t)$

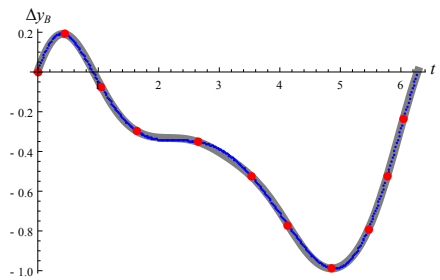


(b) Knee joint function $\Delta y_B = f_B(t)$

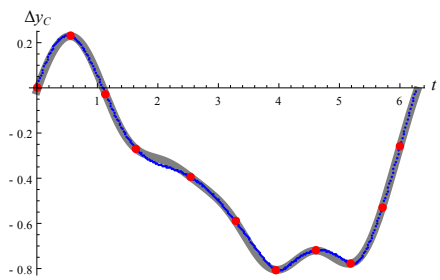


(c) Ankle joint function $\Delta y_C = f_C(t)$

Specified Function
Specified Task Points
Mechanism Generated Function

Fig. 6. The specified functions for the hip, knee, and ankle joints. These functions are plotted alongside the functions generated by the mechanisms shown in Figure 7.

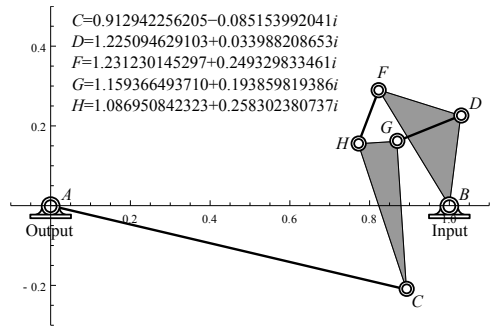


(a) 10-point hip joint $\Delta y_A$ function generator

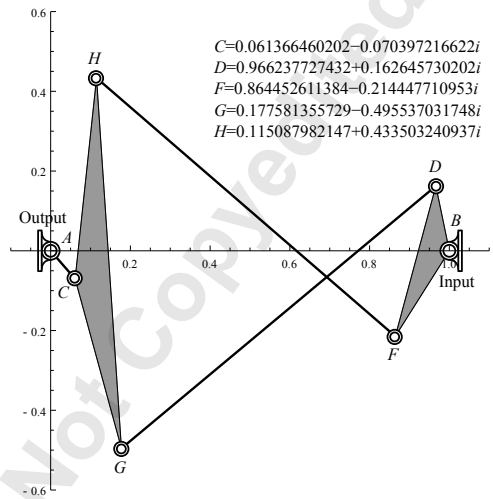


(b) 11-point knee joint $\Delta y_B$ function generator

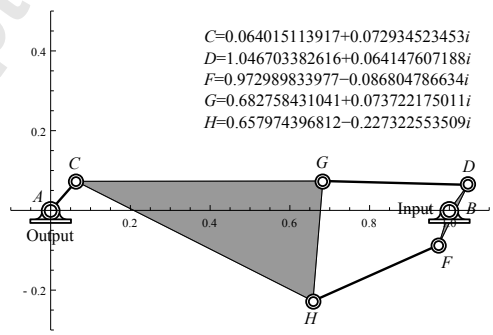


(c) 11-point ankle joint $\Delta y_C$ function generator

Fig. 7. The hip, knee, and ankle Stephenson II six-bar function generators that generate the desired functions. The input links labelled above rotate at the same constant angular velocity.

and computed as the Fourier series,

$$f(t) = \frac{1}{2}a_0 + \sum_{m=1}^{o} \left(a_m \cos(mt) + b_m \sin(mt)\right). \tag{34}$$

The Fourier coefficients for each of these functions are listed in Table 9.2. The three functions have been made to have periods of length $2\pi$ so that $t$ becomes the angle of a fully rotatable input crank with constant angular velocity that can drive all functions simultaneously. Eleven points are selected from each function which are the accuracy points that we synthesize for, displayed in Table 9.2 and Figure 6.

Example designs from the synthesis method are shown in Figure 7. All computations took place on 64×2.2GHz processors. Information on each computation is given in Table 3. Notice that the Stephenson II six-bar linkage can have either the binary link or the ternary link as input. The treatment of both cases is nearly identical. Interestingly, for the three example functions designed in this paper, we found several 11-point mechanisms when the ternary link was taken as the input and no 11-point mechanisms when the binary link was taken as the input.

Table 3 presents the number of *linkage solutions*, which are the homotopy solutions that corresponded to physical linkage designs. *Design candidates* are the linkage solutions where the solution pairs and cognate triples were identified. As well, design candidates were subjected to a maximum and minimum constraint on the size of their link lengths. Each design candidate was analyzed according to the performance verification routine described in Section 9. Table 3 also lists the number of 9-, 10- and 11-point mechanisms, see Section

Journal of Mechanisms and Robotics. Received March 09, 2015;
Accepted manuscript posted July 23, 2015. doi:10.1115/1.4031124


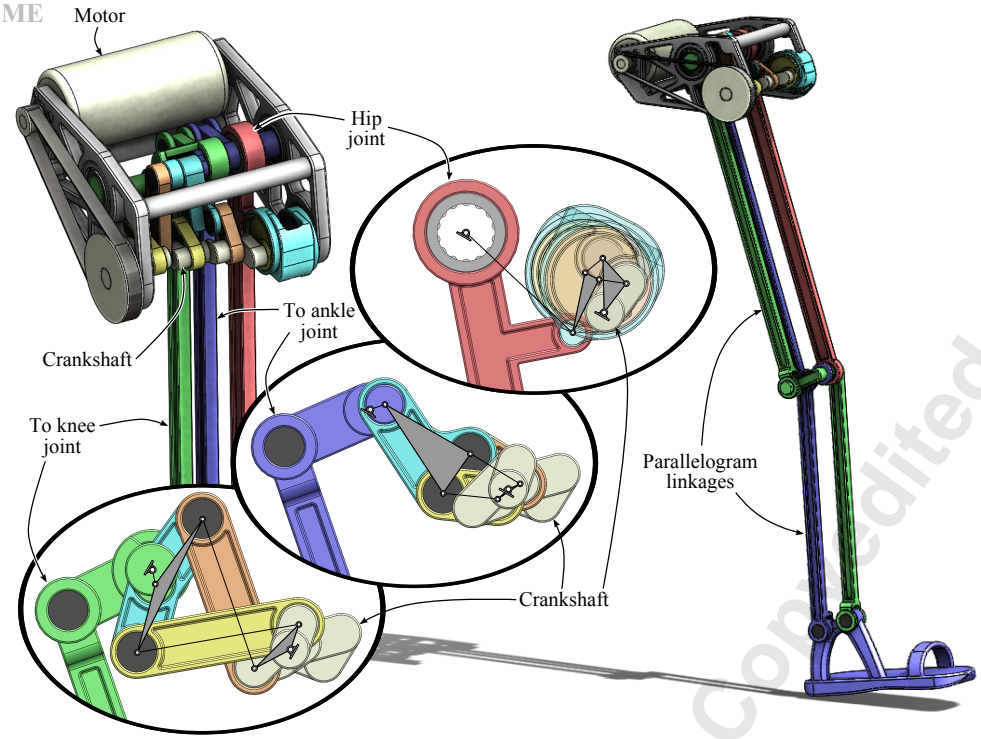


Fig. 8. Solid model of the hip, knee, and ankle function generators integrated into a humanoid walker. The schematics of Figure 7 overlay their physical embodiments for each function generator.

9.3. The *synthesis computation time* reports how long the parameter homotopy took to compute, while *analysis computation time* reports the how long it took to solve forward kinematics, sort configurations into trajectories, and identify the number of accuracy points on each trajectory.

The three linkages shown in Figure 7 were used in the design of a prototype device that creates the desired walking motion, see Figure 8. The three function generators package compactly near the hip where they are driven by a single crankshaft which serves as the input link for all three linkages. The hip joint function generator drives the hip joint directly. The motions of the knee and ankle function generators are passed down the leg chain by parallelogram linkages.

## 11 Conclusions

This paper presents a computational design procedure for Stephenson II function generators to achieve 11 coordinated input-output angles. The synthesis equations form a system of 10 eighth degree polynomials, that have a multi-homogeneous root count of 264,241,152. The polynomial homotopy software BERTINI found a general set of roots for these equations, which was then used to construct a parameter homotopy that efficiently solves the synthesis equations in about two hours on 64×2.2GHz processors.

This parameter homotopy can be executed for any set of 11 accuracy points and yields over one million solutions from which physical linkage designs, solution pairs, and cognate triples must be identified and then analyzed to determine feasible designs.

This design methodology relies on the solution of a large polynomial system and generates a large number of linkage candidates, most of which are not useful designs. In the example provided, the hip, knee, and ankle functions yielded a total of 11,182, 8,930, and 9,427 candidate designs, respectively, considering both binary and ternary driving cranks. Of these 51, 28, and 6, respectively, were feasible designs that reached the 11 required accuracy points. If the designer accepts feasible designs that reach 9 and 10 accuracy points as well, then the total number of available designs becomes 379, 382, and 62, respectively.

## Acknowledgements

This authors gratefully acknowledge the support of National Science Foundation under grant CMMI 1066082 and the assistance of Prof. Timothy Rupert and Dr. Zhiliang Pan with computations on the UC Irvine High Performance Computing Cluster.

## References

[1] Svoboda, A., 1948, *Computing Mechanisms and Linkages*, McGraw-Hill, New York, NY.

[2] Shimojima, H., and Lian, J. G., 1987, "Dimensional synthesis of dwell function generators (On 6-link Stephenson Mechanisms)", *JSME International Journal*, 30(260):324–329.

[3] Yao, Y., and Yan, H., 2003, "A new method for torque balancing of planar linkages using non-circular gears", *Proceedings of the Institution of Mechanical Engi-*

Journal of Mechanisms and Robotics. Received March 09, 2015;
Accepted manuscript posted July 23, 2015. doi:10.1115/1.4031124


*neers, Part C: Journal of Mechanical Engineering Science* 217(5):495–503.

[4] Freudenstein, F., 1954, "An analytical approach to the design of four-link mechanisms," *Transactions of the ASME*, 76:483–492.

[5] Dhingra, A. K., Cheng, J. C., and Kohli, D., 1994, "Synthesis of six-link, slider-crank and four-link mechanisms for function, path and motion generation using homotopy with m-homogenization", *Journal of Mechanical Design*, 116(4):1122-1131.

[6] Plecnik, M., and McCarthy, J. M., 2015, "Controlling the Movement of a TRR Spatial Chain with Coupled Six-bar Function Generators for Biomimetic Motion," *Proceedings of the ASME 2015 IDETC/CIE Conference*, Paper No. DETC2015-47876, August 2–5, 2015, Boston, Massachusetts.

[7] Bates, D. J., Hauenstein, J. D., Sommese, A. J., and Wampler, C. W., 2014, *Bertini: Software for Numerical Algebraic Geometry*, Available at bertini.nd.edu with permanent doi: dx.doi.org/10.7274/R0H41PB5.

[8] Bates, D. J., Hauenstein, J. D., Sommese, A. J., and Wampler, C. W., 2013, *Numerically Solving Polynomial Systems with Bertini*, SIAM Press, 352pp.

[9] Hartenberg, R. S., and Denavit, J., 1964, *Kinematic Synthesis of Linkages*, McGraw-Hill, New York, NY.

[10] Erdman, A. G., Sandor, G. N., and Kota, S., 2001, *Mechanism Design: Analysis and Synthesis*, Prentice Hall, Upper Saddle River, NJ.

[11] McCarthy, J. M., and Soh, G. S., 2010, *Geometric Design of Linkages, 2nd Ed.*, Interdisciplinary Applied Mathematics, Vol. 11, Springer-Verlag, New York.

[12] Svoboda, A., 1944, U. S. Patent No. 2,340,350, "Mechanism for Use in Computing Apparatus," February 1.

[13] McLarnan, C. W., 1963, "Synthesis of six-link plane mechanisms by numerical analysis", *Journal of Engineering for Industry*, 85(1):5-10.

[14] A. V. Mohan Rao, A. G. Erdman, G. N. Sandor, V. Raghunathan, D. E. Nigbor, L. E. Brown, E. F. Mahardy, and E. D. Enderle, 1971. "Synthesis of multi-loop, dual-purpose planar mechanisms utilizing Burmester theory", In *Proceedings of the 2nd OSU Applied Mechanism Conference*, Paper No. 7, October 7–8, Stillwater, Oklahoma.

[15] Liu, A., Shi, B., and Yang, T., 1995, "On the kinematic synthesis of planar linkages with multi-loops," *Proceedings of the Ninth World Congress on the Theory of Machines and Mechanisms*, August 29–September 2, Milan, Italy, pp. 95–97.

[16] Simionescu, P. A., and Alexandru, P., 1995, "Synthesis of Function Generators Using the Method of Increasing the Degree of Freedom of the Mechanism," *Proceedings of the Ninth World Congress on the Theory of Machines and Mechanisms*, August 29–September 2, Milan, Italy, pp 139–143.

[17] Akçali, I. D., 1995, "Modular Approach to Function Generation," *Proceedings of the Ninth World Congress on the Theory of Machines and Mechanisms*, August 29–September 2, 1995, Milan, Italy, pp 1440–1444,

[18] Kinzel, E. C., Schmiedeler, J. P., and Pennock, G. R., 2007, "Function generation with finitely separated precision points using geometric constraint programming", *Journal of Mechanical Design*, 129(11):1185-1190.

[19] Hwang, W. M., and Chen, Y. J., 2010, "Defect-Free Synthesis of Stephenson-II Function Generators", *Journal of Mechanisms and Robotics*, 2(4):041012.

[20] Sancibrian, R., 2011, "Improved GRG method for the optimal synthesis of linkages in function generation problems", *Mechanism and Machine Theory*, 46(10):1350-1375.

[21] Plecnik, M., and McCarthy, J. M., 2014"Numerical Synthesis of Six-bar Linkages for Mechanical Computation," *ASME Journal of Mechanisms and Robotics*, Vol. 6, August.

[22] Wampler, C. W., 1996, "Isotropic coordinates, circularity, and Bézout numbers: planar kinematics from a new perspective", *Proceedings of the 1996 Design Engineering Technical Conferences*, 96-DETC/MECH-1210, Irvine, CA.

[23] Dijksman, E. A., 1976, *Motion Geometry of Mechanisms*, Cambridge University Press, 291pp.

[24] Simionescu, P. A., and Smith, M. R., 2001, "Four-and six-bar function cognates and overconstrained mechanisms", *Mechanism and machine theory* 36(8): 913-924.

[25] Roberts, S., 1875, "Three-bar Motion in Plane Space", Proceedings of the London Mathematical Society s1-7(1):14-23.

[26] Chase, T. R., and Mirth, J. A., 1993. "Circuits and branches of single-degree-of-freedom planar linkages", *Journal of Mechanical Design*, 115(2):223-230.

[27] Balli, S. S., and Chand, S., 2002, "Defects in link mechanisms and solution rectification", *Mechanism and Machine Theory* 37(9): 851-876.

Journal of Mechanisms and Robotics. Received March 09, 2015;
Accepted manuscript posted July 23, 2015. doi:10.1115/1.4031124


**List of Figures**

1 (a) A Stephenson II linkage in its reference configuration and (b) a Stephenson II linkage displaced from its reference configuration drawn with dotted lines. . . . . 2
2 (a) Link vectors of the Stephenson II linkage and (b) link vectors in the $j^{\text{th}}$ displaced configuration. . . . . 3
3 Three Stephenson II cognate function generators shown in a single overconstrained mechanism. The three cognate mechanisms are comprised of pivots $\{A,B,C,D,G,H,F\}$, $\{A,B,C,D,G',H',F'\}$, and $\{A,B,C,F',G'',H'',F\}$. . . . . 5
4 The coupler curve traced by $C$ as part of the four-bar $DGHF$ is the same for two additional cognate linkages $DG'H'F'$ and $F'G''H''F$. . . . . 5
5 A humanoid leg is modelled as a planar 3R chain where $l_1 = 18.7$ and $l_2 = 14$. . . . . 7
6 The specified functions for the hip, knee, and ankle joints. These functions are plotted alongside the functions generated by the mechanisms shown in Figure 7. . . . . 9
7 The hip, knee, and ankle Stephenson II six-bar function generators that generate the desired functions. The input links labelled above rotate at the same constant angular velocity. . . . . 9
8 Solid model of the hip, knee, and ankle function generators integrated into a humanoid walker. The schematics of Figure 7 overlay their physical embodiments for each function generator. . . . . 10

Journal of Mechanisms and Robotics. Received March 09, 2015;
Accepted manuscript posted July 23, 2015. doi:10.1115/1.4031124


**List of Tables**

1 Fourier coefficients for walking gait joint angle functions. . . . . 8
2 Task points for each example function. Values below are given in degrees and must be converted to radians in order for $f_A(t)$, $f_B(t)$, and $f_C(t)$ to evaluate properly. . . . . 8
3 . . . . . 8